Enhanced Phenol Steam Reforming for Selective Hydrogen Production Using Nickel Modified Bimetallic Zinc Titanate Nanocomposite
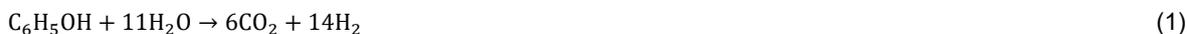
Khaled Saeed Baamran, Muhammad Tahir*, Beenish Tahir, Hajar Alias, Mohd Azizi Che Yunus

Department of Chemical Engineering, School of Chemical and Energy Engineering, Faculy of Engineering, Universiti Teknologi Malaysia (UTM), 81310 Skudai, Johor Bahru, Johor, Malaysia.
mtahir@cheme.utm.my

Highly reducible Ni/TiO_2 modified $ZnTiO_3$ composite was synthesized through hydrothermal approach and tested through phenol steam reforming (PSR) for hydrogen production. The activity tests were conducted in a continuous flow reactor to determine the effect of bi-metal modified $ZnTiO_3$ support on PSR reaction. The highest phenol conversion and H_2 yield were achieved using TiO_2 loaded with 10 % and dispersed over $ZnTiO_3$. The phenol conversion and H_2 selectivity of 89.1 % and 75.6 % were obtained in the 10 % Ni/TiO_2-$ZnTiO_3$ catalyst, and were only 43.8 % and 13.8 % in the 10 % Ni/TiO_2 catalyst. The enhanced activity for selective hydrogen production was due to strong Ni interaction with TiO_2 metal oxide and $ZnTiO_3$ perovskite with larger exposed active sites availability. Among the operating parameters, 700 °C, 5/95 wt% phenol/water, and 1 atm were the optimum conditions for maximum H_2 production. The composite catalyst provides a higher catalyst in terms of phenol conversion and H_2 evolution with excellent durability. Ni/TiO_2 modified $ZnTiO_3$ composite is a promising reforming catalyst for H_2 production and can be further employed in cleaner energy production and other environmental applications.

1. Introduction

Steam reforming (SR) using organic compounds derived from biomass with high hydrogen (H_2) level such as alcohols (Mulewa et al., 2017) and phenol as a bio-oil component is a promising technology for H_2 production from renewable sources (Liang et al., 2017). In SR processes, phenol steam reforming (PSR) is a complex process in terms of a network of side reactions as depicted in Eqs (1-4) and its endothermic nature that contributes to formation of by-products like CO, CO_2, and most important and detrimental, coke.

$$C_6H_5OH + 11H_2O \rightarrow 6CO_2 + 14H_2 \tag{1}$$

$$C_6H_5OH + 5H_2O \rightarrow 6CO + 8H_2 \tag{2}$$

$$CO + H_2O \leftrightarrow CO_2 + H_2 \tag{3}$$

$$2CO \rightarrow C + CO_2 \tag{4}$$

Several catalytic systems such as MgO, ZrO_2, CeO_2 and La_2O_3 have been investigated in PSR. Besides, several precious/noble metals such as Rh, Pt and Pd have been investigated in PSR. Among them, highest stability with minimal coke deposition has been reported using Rh as active metal. Rh is expensive with less availability, so the use of such noble metals is unattractive for industrial purposes (Gao et al., 2018). In reforming processes, research efforts have been directed towards transition metals such as Ni due to it is exceptional activity particularly when it is highly dispersed on supports, and it is relatively low cost and availability in nature compared to noble metals (Constantinou et al., 2009).

Numerous research studies have been investigated in Ni-based catalysts for PSR such as Ni/ZrO_2, $Ni/\gamma-Al_2O_3$ and Ni/CeO_2 (Nabgan et al., 2016). However, using high temperature, Ni-based systems have limitations such as large amounts of carbon formation, resulting in deactivation, instability and loss of dispersion. To this obstacle, structured bi-metal and reducible supports could be an appropriate way to improve metal dispersion due to the metal-support interaction (Mulewa et al., 2017). In this view point, Nabgan et al. (2016), concluded that reducible materials which include CeO_2 and ZrO_2 dispersed Ni exhibited minimal carbon formation compared with other oxides such as Al_2O_3 and La_2O_3.

During the past years, titanium dioxide (TiO_2) has been widely considered due to its dual effects such as working as active metal and reducible support. It has exceptional features which includes excessive availability in nature, high stability, nontoxic (Tahir et al., 2016) and cost-effective (Tahir et al., 2017). The SR processes such as ethanol steam reforming and PSR have been investigated using Ni-modified TiO_2 catalyst and reported good efficiency for H_2 production (Baamran et al., 2019). However, it has limitations such as higher carbon formation, and lower selectivity for continuous H_2 production (Díaz-Pérez et al., 2018). Abbas et al. (2018), reported that the metal-support interaction between Ni/TiO_2 NPs and Co_3O_4 revealed excellent stability and activity for H_2 production with coke resistance compared to Ni/TiO_2 NPs. Within this perspective, bi-metal oxides such as perovskite-based catalysts co-loaded with TiO_2 as a composite catalyst would be an attractive technique in PSR (Nabgan et al., 2016). Zinc titanate ($ZnTiO_3$) has been attracted considerable attention in photocatalysis reactions due to its redox properties, compositional flexibility, chemical stability, and effective-cost material. The fabrication of bi-metal support in the form of $ZnTiO_3$ perovskite and embedded with Ni would be promising in PSR reaction.

Synthesis of NiO and TiO_2 promoted $ZnTiO_3$ composite for continuous hydrogen production through PSR has been investigated. The catalysts samples were synthesized using two steps hydrothermal methods. The crystallinity, morphology and structure were analysed using XRD, FE-SEM, EDX and TEM. The role of Ni and TiO_2 with their bimetallic interaction with $ZnTiO_3$ has been systematically investigated. The effect of operating temperature and reaction mechanism is further investigated based on experimental results.

2. Experimental

2.1 Catalyst preparation and characterization

The chemicals used for the synthesis of $ZnTiO_3$ were zinc nitrate and titanium (IV) isopropoxide purchased from Sigma-Aldrich. The hydrothermal method was used for in-situ synthesis of $ZnTiO_3$ and TiO_2 NPs. In a typical procedure, 0.2 mole of zinc nitrate dispersed in 50 mL deionized water were mixed with ammonium hydroxide until a pH 10 was achieved. Afterwards, 0.1 moles of titanium precursor were added to zinc solution under stirring. The mixture was transferred to 100 mL Teflon autoclave and heated at 120 °C for 12 h and finally dried overnight at 100 °C. The product obtained was calcined for 5 h at 750 °C and then cooled down naturally. The product obtained was named as TiO_2 dispersed $ZnTiO_3$. For the synthesis of Ni-loaded TiO_2-$ZnTiO_3$ samples, impregnation method was employed. Briefly, different amounts of nickel nitrate (e.g., 5, 10, and 15 wt%) were added separately in 100 mL deionized water with 1 g of support (TiO_2-$ZnTiO_3$). The solution was stirred for 5 h at ~25 °C and dried in an oven for 24 h. Then, the final cake was calcined at 500 °C for 3 h before it was used. The materials obtained were characterized using different techniques such as X-ray diffraction (XRD), and Field Emission Scanning Electron Microscopy (FE-SEM) to determine crystal structure and morphology. For spent samples, an energy dispersive spectrometer (EDX) was utilized to determine the amount of carbon formation after the PSR reaction integrated with a high-resolution transmission electron microscope (HR-TEM) to investigate the surface morphology of the used samples.

2.2 Activity test for PSR

The reactions of steam reforming of phenol over TiO_2, Ni loaded TiO_2 and Ni loaded TiO_2-$ZnTiO_3$ catalysts were performed in a fixed bed reactor. The stainless reactor with outer diameter 0.012 m was employed. K-type thermocouple was used to measure reactor temperature. The feed mixture of phenol/water was passed through the reactor using a syringe pump. The carrier gas employed was N_2 (purity, 99.99 %, flowing at 10 mL/h. The feed was pre-heated at 250 °C before entering the reactor. Reactor temperature of 700 °C and N_2 flow rate of 10 mL/h, 5/95 wt% phenol/water concentration were used in all the experiments. The reaction was conducted at atmospheric pressure and products were analyzed using an online gas chromatography (GC) equipped with a thermal conductivity detector (TCD) and installed with a 30m×0.53mm Carboxen Plot 1010 capillary column. For phenol liquid samples, a GC system equipped with 0.53mm×30m DB-Wax capillary column was used. The catalytic quantitative analysis was evaluated according to equations reported by Baamran et al. (2019).

3. Results and discussion

3.1 Catalyst characterization

XRD patterns of TiO_2, 10 % Ni/TiO_2 NPs, TiO_2-$ZnTiO_3$ and 10 % Ni/TiO_2-$ZnTiO_3$ composite are depicted in Figure 1a-b. The pure TiO_2 NPs were in anatase phase positioned at 2θ of 25.22°, 37.10°, 47.98°, and 53.99°, which are corresponding to (101), (004), (200) and (105) planes. When Ni dispersed on TiO_2 NPs, the same peaks of TiO_2 NPs appeared beside a 2θ at 43.10° ascribing to NiO. The diffraction peaks of composite samples (TiO_2-$ZnTiO_3$) were seen in stronger and sharper peaks compared to pure TiO_2 NPs due to interacting with $ZnTiO_3$ perovskite. The composite sample has (104), (110), (024), (116) and (214) planes, which are located at 2θ of 33.07°, 35.54°, 49.38°, 53.99° and 62.34°. TiO_2-$ZnTiO_3$ loaded 10 % Ni were observed to have the same peaks as pure TiO_2-$ZnTiO_3$ in addition to NiO peaks placed at 2θ of 37.10° and 43.10°, which are corresponding to (101) and (012) planes. Zn appears in cubic perovskite $ZnTiO_3$, pointing out of a well-controlled synthesis using hydrothermal method resulted in growing perovskite structure of $ZnTiO_3$.
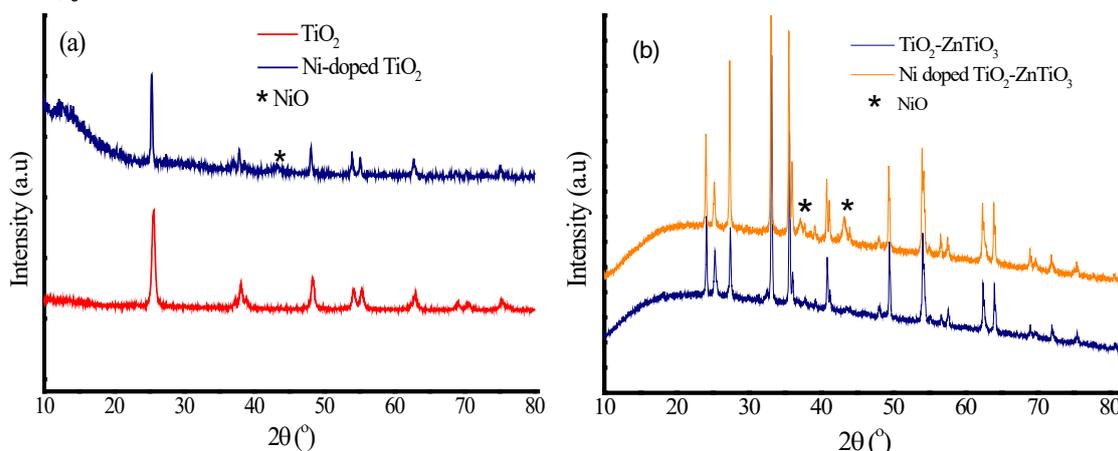

Figure 1: (a) X-ray diffraction patterns of TiO₂ and Ni-doped TiO₂ samples; (b) XRD patterns of TiO₂-ZnTiO₃ and Ni doped TiO₂-ZnTiO₃ composite samples

FE-SEM analysis was used to investigate the morphology and microscopic structure of catalysts as illustrated in Figure 2a-b. Clearly, Ni/TiO_2 NPs are in uniform size with nearly a spherical shape as depicted in Figure 2a. Figure 2b shows the morphology of TiO_2 NPs and $ZnTiO_3$ perovskites as a nanocomposite embedded Ni. The spherical shape of TiO_2 NPs is evenly distributed over $ZnTiO_3$ cubic perovskite. The Ni/TiO_2-$ZnTiO_3$ composite is a cluster of nanoparticles and perovskites. It can be categorized as a heterogeneous Ni/TiO_2-$ZnTiO_3$ nanocomposite. Ni is impossible to be identified due to its little tiny amount and high dispersion among the catalyst surface because the metal supports interaction.
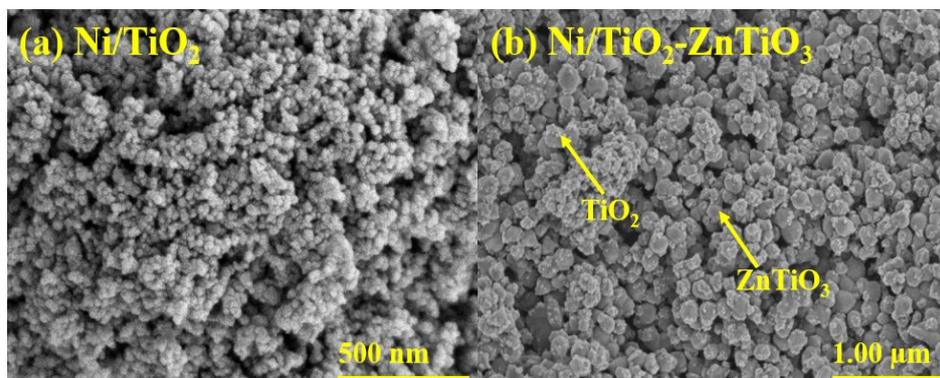

Figure 2: FE-SEM analysis of (a) Ni-doped TiO₂; (b) Ni-doped TiO₂-ZnTiO₃ composite samples

3.2 Phenol steam reforming for hydrogen production

The nature of support structure and metal loading are important factors affecting the catalytic performance. A preliminary test over mono/bi-metal supports (TiO_2/ TiO_2-$ZnTiO_3$) and supports loaded to optimal amounts of

Ni was carried out to investigate the catalytic performance. The samples were prepared using hydrothermal assisted impregnation methods and all the experiments were conducted using temperature 700 °C, feed flow rate 10 mL/h, catalyst loading 0.3 g, and feed concentration of 5/95 wt% of phenol and water. In a homogeneous reaction, 2.93 % phenol conversion and 2.18 % H_2 yield were obtained, confirming negligible phenol conversion and hydrogen production in the absence of catalyst. When experiments were conducted in the presence of catalysts, phenol conversion and hydrogen yield were significantly increased. In this perspective, using pure TiO_2 support, 43.28 % phenol conversion and 13.2 % hydrogen yield were obtained. This confirms TiO_2 has dual function such as can work as an active metal and also as a support due to its reducible properties. Using TiO_2-$ZnTiO_3$ catalyst, phenol conversion and hydrogen yield were further increased, which are 57.6 % phenol conversion and 68.32 % hydrogen yield. Besides, other products obtained were 12.87 % CO and 14.6 % CO_2. The selectivity for H_2, CO and CO_2 of 68.09, 10.69 and 20.52 %, were obtained, which returns to the support structure with lattice network and the interaction of support metals that dictate electronic transports among support metals, also due to the thermodynamic feasibility of PSR, water gas shift (WGS), and the reverse of WGS (RWGS) reactions as shown in Eqs (1-3). An access to active sites and improved activity of composite support were obtained.

Catalysts screening was conducted in the range 5 to 15 wt% Ni-loading and applied to the composite support. Evidently, the catalytic activity was enhanced with 5 wt% Ni and 83.2 % phenol conversion and ~68 % H_2 yield were obtained. This improvement of catalytic activity was observed up to 10 wt% Ni which accordingly was considered as the optimal Ni loading. This can be attributed to the presence of active sites because of good dispersion and strong interaction among the components. On the other hand, adding higher Ni loading such that 15 wt% Ni, a decline in phenol conversion from 89.10-82.63 % and H_2 yield 75.60-65.78 % were observed, which can be returned to aggregation of Ni particles that reduce the dispersion of metal. TiO_2 NPs supported the optimal loading of Ni (10 wt%) exhibited good catalytic activity as shown in Figure 3a. However, compared to Ni/TiO_2-$ZnTiO_3$, higher activity was observed in the composite sample due to several reasons. The high metal dispersion among the lattice network of composite catalysts will assist in further access of active sites. Consequently, promoted activity and stability for phenol conversion and products (H_2 and CO_2) yield were observed in Ni-doped TiO_2-$ZnTiO_3$ compared to Ni-doped TiO_2 as depicted in Figure 3a-3b. Interestingly, CO yield was 9.78 % in 10 % Ni/TiO_2, reduced to 6.51 % in 10 % Ni/TiO_2-$ZnTiO_3$ composite. Synthesizing TiO_2 nanoparticles with $ZnTiO_3$ in a single step are beneficial for stimulating catalytic activity and hydrogen production selectivity. Using 10 % Ni-doped TiO_2-$ZnTiO_3$ catalyst highest catalyst activity for phenol conversion and hydrogen production was achieved. Besides, production of CO was minimized over the composite catalyst, evidently due to hindering carbon formation, resulting in highest stability over time on stream. 10 % Ni/TiO_2-$ZnTiO_3$ composite catalyst was determined to be of optimum structure and formulation. The highest performance of composite catalyst with continuous hydrogen production was due to lower coke formation due to Ni and TiO_2 interaction and their good dispersion over $ZnTiO_3$ perovskite composites.
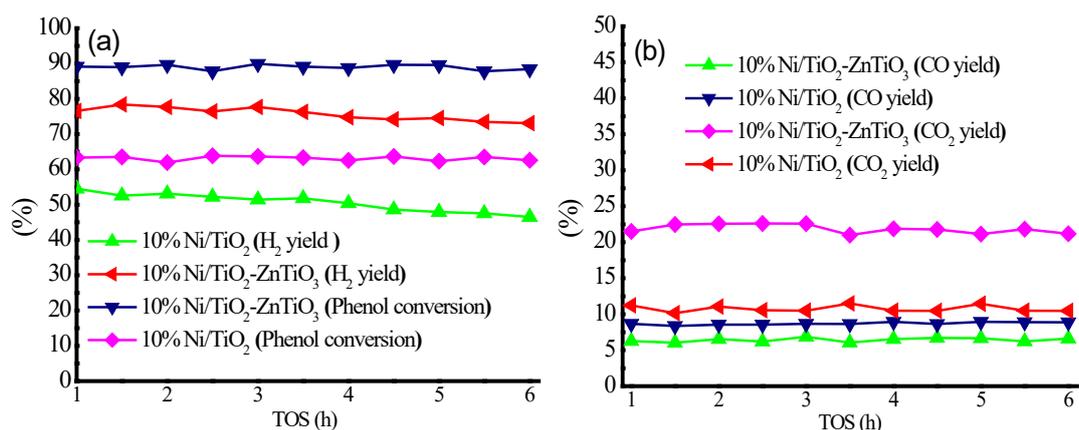

Figure 3: (a) Phenol conversion and hydrogen yield, and (b) Yield of CO and CO_2 (700 °C, catalyst loading 0.3 g, feed flow rate 10 mL/min, phenol feed 5 wt% and pressure 1 atm)

The effect of temperature ranging 600 to 800 °C for the production of H_2, CO and CO_2 have been demonstrated in Figure 4. Figure 4a shows the effect of temperature on hydrogen yield. Obviously, production of hydrogen was increased by increasing reaction temperature. The H_2 yield was increased from ~58 % at temperature 600 °C to ~88 % at reaction temperature of 800 °C. This confirms that PSR is an endothermic reaction which is increasing by providing more input energy. Besides, continuous production of hydrogen was

obtained over time on stream (50 h), obviously, due to high stability of composite catalyst as shown in Figure 4b.
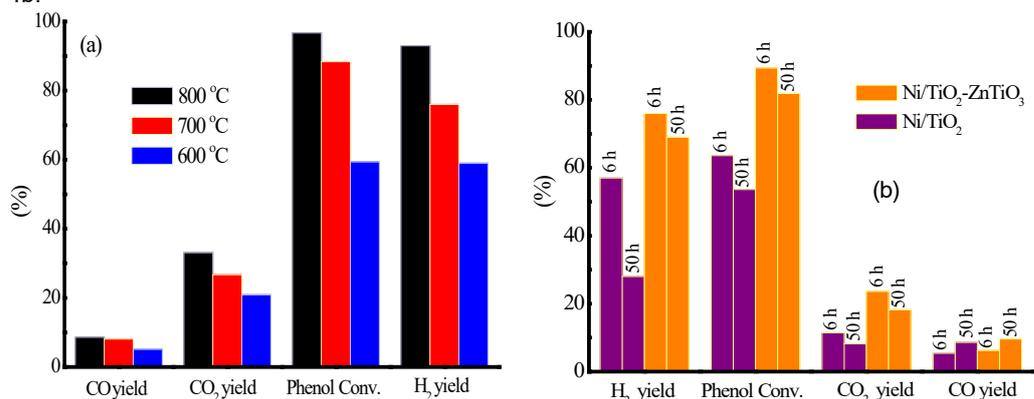

Figure 4: (a) *Effect of temperature on product yield and phenol conversion using Ni/TiO₂-ZnTiO₃ catalyst; (b) Stability test of 10 % Ni/TiO₂, and 10 % Ni/TiO₂-ZnTiO₃ on product yield and phenol conversion*

Phenol conversion was also significantly increased by increasing reaction temperature as demonstrated in Figure 4a. The highest phenol conversion of ~96 % was obtained at reaction temperature of 800 ºC, evidently due to providing more input energy because of the endothermic nature of reaction. Figure 4a also illustrates the production of CO and CO_2 at different reaction temperatures. Using lower temperature (600 ºC), small amounts of CO and CO_2 were produced, which are significantly enhanced by increasing temperature from 600 to 800 ºC. This confirms direct effect of reaction temperature on the production of CO and CO_2 due to higher phenol conversion, and the feasibility of PSR, WGS, and RWGS reactions. The higher catalytic activity was due to higher NiO-dispersion at 6.5 % in the composite catalyst compared to ~4 % in Ni/TiO₂, and to the influence of ZnTiO₃ support. The metal dispersion was estimated according to equations reported by Mulewa et al. (2017) at nearly 2θ=43.10° in XRD. The presence of reducible metal oxide (TiO₂) and good interaction among the NiO, TiO₂ and ZnTiO₃ in NiO-doped TiO₂-ZnTiO₃ composite samples resulted in a high stability for more than 50 h (Figure 4b), and minimum carbon deposition as illustrated in Figure 5a which was estimated by ~5.8 wt% using EDX (Figure 5b). The formation of small carbon amounts is probably due to the Boudouard reaction (Eq (4)). However, enhanced catalyst activity towards breaking C-C and C-H bonds has promoted H_2 production. The increase in CO yield was due to activation of RWGS reaction (Tahir et al., 2017), which is feasible at high temperatures (Nabgan et al., 2016). High temperature is favourable for PSR to maximize H_2 production and phenol conversion with stability and minimum coke formation.
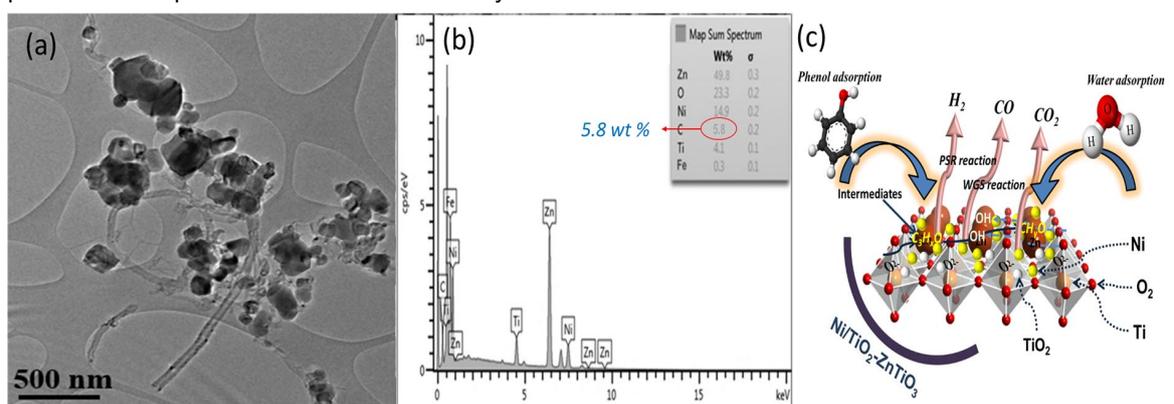

Figure 5: (a) *TEM image;* (b) *EDX elemental analysis of Ni/TiO₂-ZnTiO₃ spent sample;* (c) *Schematic for the PSR reaction mechanism on the composite catalyst*

3.3 Reaction mechanism

During phenol steam reforming reaction over Ni-doped TiO₂-ZnTiO₃ composite, a schematic mechanim has been illustrated in Figure 5c. Intermediates such as methane were not formed during the operating parameters investigation. PSR and RWGS reactions are more favorable at high temperatures. Under the limitation of the applied operating conditions, phenol decomposition and methanation reactions would not much affect the

global mechanism of this process since no methane was obtained and phenol is mostly consumed by the reactions of PSR, WGS and RWGS (Eqs (1-3)). The metal and support are the sites where the reactants (C_6H_5OH and H_2O) are adsorbed. The formed species at the catalyst surface is thereafter reacted with steam (H_2O)/hydroxyls that are usually activated on supports. Phenol molecule was activated over Ni-metal particles as active sites and also due to the basic nature of catalyst support (TiO_2-$ZnTiO_3$) to generate the intermediate products (C_3H_xO or CH_yO). NH_4OH provides strong basicity to support, where the anions like O_2- existing at edges and corners, are in charge of the strong basic sites coordination. The mobile oxygenates provided by the catalyst support are engaged in phenol steam reforming process for gaseous products and inhibit coke deposition.

4. Conclusions

Structured Ni/TiO_2-loaded $ZnTiO_3$ composite were successfully synthesized via hydrothermal and impregnation methods and tested for H_2 production from PSR. Highest hydrogen production over Ni-TiO_2-$ZnTiO_3$ composite was achieved compared to NiO/TiO_2 catalyst due to metal and mono-metal oxide (TiO_2) interaction and good dispersion over cubic $ZnTiO_3$ structure.

Acknowledgements

Reference

Abbas T., Tahir M., Amin N.A.S., 2018, Enhanced metal-support interaction in Ni/Co_3O_4/TiO_2 Nanorods toward Stable and Dynamic Hydrogen Production from Phenol Steam Reforming, Industrial and Engineering Chemistry Research, 58(2), 517-530.

Baamran K.S., Tahir M., Mohamed M., Khoja A.H., 2019, Effect of support size for stimulating hydrogen production in phenol steam reforming using Ni-embedded TiO_2 nanocatalyst, Journal of Environmental Chemical Engineering, 8(1), 103604.

Constantinou D.A., Fierro J.L.G., Efstathiou A.M., 2009, The phenol steam reforming reaction towards H_2 production on natural calcite, Applied Catalysis B: Environmental, 90(3-4), 347-359.

Díaz-Pérez M.A., Moya J., Serrano-Ruiz J.C., Faria J., 2018, Interplay of support chemistry and reaction conditions on copper catalyzed methanol steam reforming, Industrial and Engineering Chemistry Research, 57(45), 15268-15279.

Gao N., Han Y., Quan C., 2018, Study on steam reforming of coal tar over NiCo/ceramic foam catalyst for hydrogen production: Effect of Ni/Co ratio, International Journal of Hydrogen Energy, 43(49), 22170-22186.

Liang T., Wang Y., Chen M., Yang Z., Liu S., Zhou Z., Li X., 2017, Steam reforming of phenol-ethanol to produce hydrogen over bimetallic NiCu catalysts supported on sepiolite, International Journal of Hydrogen Energy, 42(47), 28233-28246.

Mulewa W., Tahir M., Amin N.A.S., 2017, Ethanol Steam Reforming for Renewable Hydrogen Production over La-Modified TiO_2 Catalyst, Chemical Engineering Transactions, 56, 349-354.

Mulewa W., Tahir M., Amin N.A.S., 2017, MMT-supported Ni/TiO_2 nanocomposite for low temperature ethanol steam reforming toward hydrogen production, Chemical Engineering Journal, 326(15), 956-969.

Nabgan W., Abdullah T.A.T., Mat R., Nabgan B., Gambo Y., Triwahyono S., 2016, Influence of Ni to Co ratio supported on ZrO_2 catalysts in phenol steam reforming for hydrogen production, International Journal of Hydrogen Energy, 41(48), 22922-22931.

Nabgan W., Abdullah T.A.T., Mat R., Nabgan B., Triwahyono S., Ripin A., 2016, Hydrogen production from catalytic steam reforming of phenol with bimetallic nickel-cobalt catalyst on various supports, Applied Catalysis A: General, 527(25), 161-170.

Nabgan W., Mat R., Abdullah T.A.T., Nabgan B., Gambo Y., Zakaria Z.Y., 2016, Development of a kinetic model for hydrogen production from phenol over Ni-Co/ZrO_2 catalyst, Journal of Environmental Chemical Engineering, 4(4), 4444-4452.

Tahir B., Tahir M., Amin N.A.S., 2018, Photocatalytic CO_2-Hydrogen Conversion via RWGSR over Ni/TiO_2 Nanocatalyst Dispersed in Layered MMT Nanoclay, Chemical Engineering Transactions, 63, 115-120.

Tahir B., Tahir M., Amin N.A.S., 2017, Photocatalytic Carbon Dioxide and Methane Reduction to Fuels over La-Promoted Titanium Dioxide Nanocatalyst, Chemical Engineering Transactions, 56, 1123-1128.

Tahir M., Tahir B., Amin N.A.S., 2017, Photocatalytic Reverse Water Gas Shift CO_2 Reduction to CO over Montmorillonite Supported TiO_2 Nanocomposite, Chemical Engineering Transactions, 56, 319-324.